MINISTRY OF EDUCATION, RESEARCH AND SPORTS

UNIVERSITY „BABEŞ – BOLYAI”
CLUJ – NAPOCA

FACULTY OF PHYSICS

Cristian Daniel Tudoran

GENERATION AND CHARACTERIZATION OF HIGH FREQUENCY PLASMAS. APPLICATIONS

- Summary of the thesis -

Scientific supervisor,
Prof. Dr. Sorin Dan ANGHEL

str. Mihail Kogălniceanu nr. 1, 400084 Cluj-Napoca, România
http://www.ubbcluj.ro

2011

Summary

KEY WORDS:

Radiofrequency plasma

Microwave plasma

Surface engineering

Sintering of metallic powders

Plasma sterilization

1. INTRODUCTION

Currently, the areas of study and application for the high-frequency plasmas include applications in the following domains: bio-medical, plasma displays, sources of particles and/or ionizing radiation, chemical analysis systems, gas analyzers, photodetectors, lasers, dynamic microwave processing equipment, cold plasma process reactors, propulsion systems, air flow control systems (with applications in aerodynamics), materials processing and environmental applications, in many cases the non-thermal plasma is generated under atmospheric pressure conditions using low-power generators, sometimes with output power levels not exceeding a few tens of watts. Modern equipment for plasma generation is usually based on switching technology implemented with MOSFET type transistors (Metal Oxide Semiconductor Field Effect Transistor) or IGBT (Insulated Gate Bipolar Transistor) transistors.

What new element can bring a doctoral thesis in plasma physics in 2011? Based on the observation that the border between the thermal effects and the non-thermal effects produced by the plasma under atmospheric pressure conditions on a material or living tissue is extremely fragile, this thesis aims to deepen the concepts of non-thermal plasma generation and their effects on different materials and biological structures. Thus, the physical realization of some RF plasma generators to obtain the two types of effects and the study of these effects on different materials, is a new approach from the perspective of the reviewed literature. Even though the conversion efficiency of our generators is not very high, designing the laboratory apparatus for surface treatment experiments with non-thermal plasma allowed us to obtain a series of interesting results and conclusions about the effects of cold plasma on the surface properties and microbiological structures.

2. GENERATION OF HIGH FREQUENCY PLASMAS

To generate the plasma, usually there are two types of systems: self-resonant amplifiers and liniar type RF amplifiers which are based on a signal generator module followed by a couple of amplifying stages. In the self-resonant type generators, the plasma together with output coil are an integral part of the oscillator circuit, and to achieve the maximum power transfer, the output impedance must be matched to the load impedance [2.1], usually by means of capacitive elements. In this case, the ignition of the plasma is accompanied by a drop in the frequency of the generator. For this reason, the frequency of the generator must be precisely maintained in the limits of the industrial frequency domains. In case of the generatos based on crystal oscillators, the frequency is fixed and the signal is being sent through a cable to the plasma chamber assembly.

2.1 Design and construction of the „PLAS–01" radiofrequency (4 MHz) plasma generator

The "PLAS-01" generator is based solely on general purpose semiconductor components, which are relatively easy to procure [2.5]. The complete scheme of the experimental model of this high frequency plasma generator can be divided into the following modules: power supply module, pilot oscillator (a 4 MHz internal crystal driven oscillator), preamplifier stage, driver module, final power stage and fault protection module. Their function is as follows:

1) The power supply module supplies the other modules of the generator: +5 V and + 12 V for the pilot oscillator and preamplifier stage and +300 V for the final power stage. The two low level voltages are filtered and stabilized and the high voltage (+300 V) is filtered by a L-C π-type filter.
2) The pilot oscillator module is based on a TTL integrated circuit called CDB405 (7405) which is a hex inverter with open collector outputs. Its task is to generate the primary square wave drive signal. The oscillator is driven by a 4 MHz quarz crystal.
3) The preamplifier and driver module is based on the TPS2814P MOSFET driver I.C, which can deliver a square wave drive signal with an intensity up to 2 A, necessary for the switching of the power MOSFET transistor in the final stage.
4) The final power stage is based around a MOSFET switching power transistor (IRFBC40).
5) The fault protection module protects the plasma generator in two fault conditions: over current and over voltage, blocking the drive signal to the final power stage.

   The block logic schematics of the "PLAS-01" generator is given in figure 1.

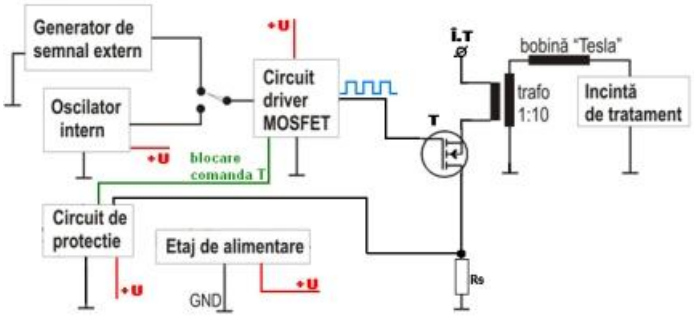

Figure 1. The block logic schematics of the "PLAS-01" generator.

This generator was used also in non-thermal plasma experiments, coupled to a Dielectric Barrier Discharge (DBD) chamber. The first experimental discharge chamber was built using rectangular pieces of glass, bonded together with expoxy resin. In figure 2 a and b we can observ such a DBD discharge chamber, working at a frequency of 1.6 MHz. This chamber was used for a preliminary sets of studies regarding the interaction of the cold plasma with the surface of some polymeric materials. [2.3].

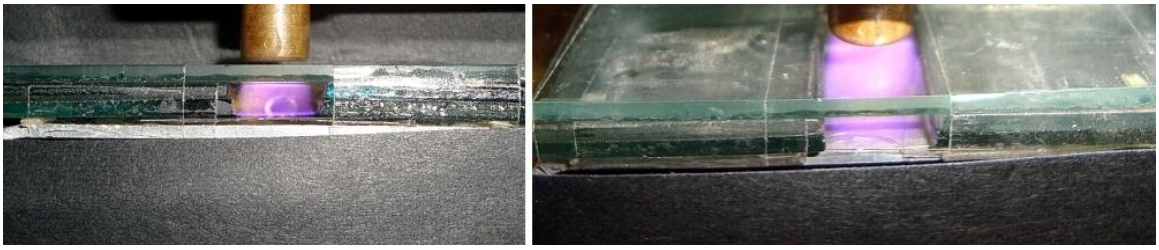

a **b**

Figura 2. The DBD generated with the "PLAS-01" generator: **a** – frontal view, **b** – top view.

2.2 Design and construction of the „PLAS–02" radiofrequency (1.7 MHz) plasma generator

This second generator called "PLAS-02" was designed and built with the ideea to perform advanced studies on non-thermal plasma interaction with the surface of materials and biological structures. It is a radio frequency power generator (250 W) based on inverter MOSFET switching technology. The final power stage is an inverter circuit configuration called a "half-bridge". We chose this configuration for two reasons [2.6]: 1) higher efficiency of an inverter compared to a classic switching circuit with only a single transistor, and 2) the inverter requires a symmetric supply voltage (U_{+}, U_{-}) with a smalled voltage amplitude, in comparison with a single transistor switch, in order to generate the plasma under atmospheric pressure conditions – this translates to a more durable system.

Figure 3 presents the block schematics of the "PLAS-02" generator. The generator contains an internal PLL type oscillator with variable frequency. The frequency can be adjusted depending on the

imposed operating conditions (the resonant frequency is dictated by the Tesla coil's natural frequency coupled to the discharge chamber assembly). The TTL complementary drive signal module takes the primary signal from the internal oscilator and forms the two comand signals for the inverter's two channels (transistors T1 and T2 on figure 4). The two complementary signals are then sent through opto-couplers to the final driver stage modules.

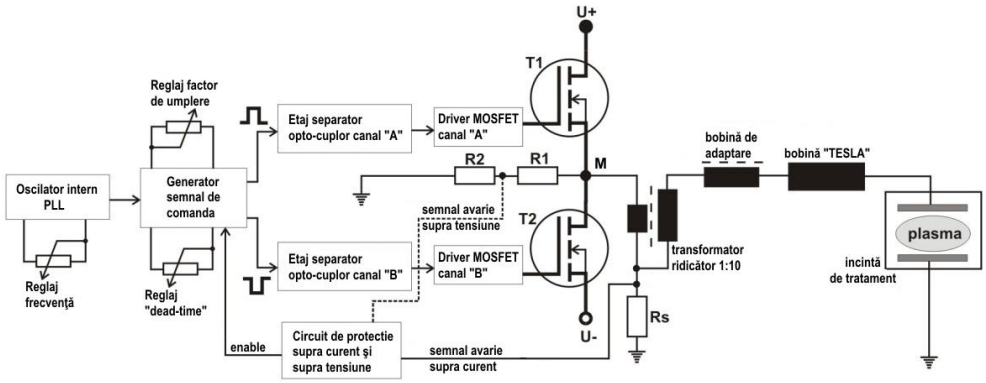

Figura 3. The block schematics of the "PLAS-02" generator.

The MOSFET driver modules are designed to provide the high intensity drive signals to the gates of the power transistors T1 and T2, figure 4. The load of the inverter power stage is the series circuit form by the step up transformer (1:10), matching coil, Tesla coil [2.4] and the discharge chamber [2.6]. The entire system is protected with a protection circuit that blocks the driver signals in case of over voltage or over current fault conditions. The DBD plasma discharge chamber is made of Plexiglas, has a rectangular shape and contains two horizontally mounted disk shaped electrodes. The electrodes are made from copper and are covered with a Teflon coating with a thickness of 1.5 mm (Figure 4 a). The gap between the electrodes can be adjusted with the help of the fine threads cut on their support rods. The plasma gas (Helium) enters the discharge chamber through a nozzle attached to one of the vertical sides of the chamber, and ventilation occurs through a series of holes made on the opposite side. The construction details of the discharge chamber are shown in figure 4 a, and figure 4 b shows the discharge chamber in operation during a diagnostic study of the generated plasma (note the optic fiber coupled to the front wall of the chamber).

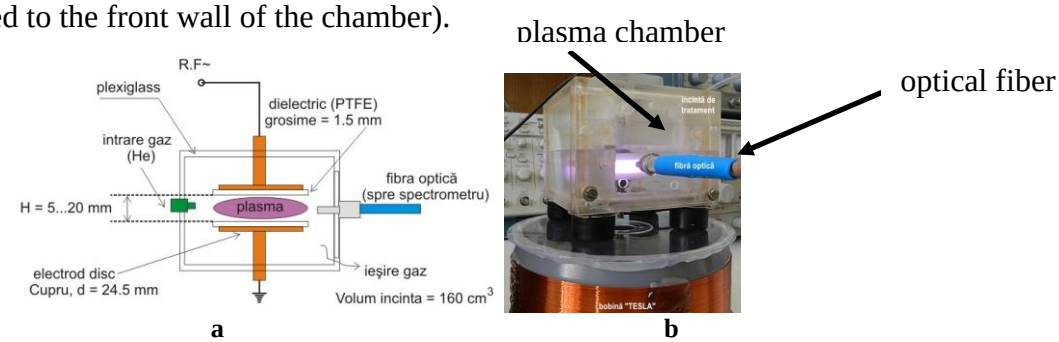

Figure 4. The plasma discharge chamber: **a** – technical details, **b** – the plasma chamber during an experiment.

2.3 Power microwave plasma generator for sintering experiments

This microwave plasma generator is located at the „Surface Engineering Laboratory" at University College Dublin, Faculty of Electrical Electronic and Mechanical Engineering. The generator was built with the purpose to carry out studies of sintering metallic powders by microwave plasma. The system consists of a rectangular waveguide section provided at one end with a Muegge type magnetron power source (6 kW, 2.45 GHz). On the opposite side of the waveguide there is a piston that enables the fine tuning of the generator in order to achieve the smallest possible reflected power coefficient during operation [2.2]. The microwave energy is coupled from the middle of the waveguide with the help of a rod type coupling loop and is driven downwards in the resonant cavity by a disk shaped antenna. The resonant cavity is a „U" shaped toroid. On the lower side of the resonant chamber, there is a piston that can move up and down in order to finely tune the chamber (Figure 5). The samples to be sintered are placed inside the resonant cavity, on the top of the tuning piston, on a support made from quartz. The generator system also has a bicolor pyrometer and a type „S" thermocouple for monitoring the temperature of the samples during the sintering process. The characterization of the microwave plasma is carried out by means of optical-spectral (OES) methods using a set of "Ocean Optics" high-resolution spectrometers.

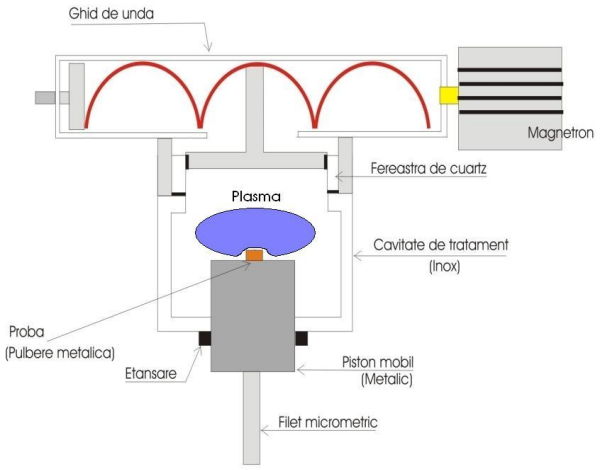

Figure 5. Technical schematic of the high power microwave plasma generator for sintering experiments.

References

[2.1] S.D Anghel, A. Simon, "Plasma de înaltă frecvență", Ed. Napoca Star, Cluj-Napoca, 2002, ISBN 973 – 647 – 060 -1

[2.2] N St J Braithwaite, "Introduction to gas discharges",Plasma Sources Sci. Technol. 9 (2000) 517

[2.3] H Conrads, M Schmidt, Plasma generation and plasma sources, Plasma Sources Sci. Technol. 9 (2000) 441–454

[2.4] Marco Denicolai, "Tesla Transformer for Experimentation and Research" -PhD Thesis, Helsinky University of Technology, 2001

[2.5] Cristian D Tudoran, “Simplified portable 4 MHz RF plasma demonstration unit”, Journal of Physics: Conference Series 182 (2009) 012034 doi:10.1088/1742-6596/182/1/012034

[2.6] Cristian.D. Tudoran, “High Frequency Portable Plasma Generator Unit For Surface Treatment Experiments”,Romanian Journal of Physics, Jan.2011, ISSN 1221-146X

3. HIGH FREQUENCY PLASMA DIAGNOSTICS AND MODELING

The measurement or determination of intrinsic physical parameters of the plasma (particle concentration, degree of ionization, the particle temperatures, etc.) is called plasma diagnostics.

The large variety of states in which plasmas exist, required the finding and developing of a series of diagnostics methods. The experimental measurements and the theoretical determinations focus mainly on the following plasma parameters: density and kinetic temperature of the charge carriers existing in the plasma(n_e, T_e, n_i, T_i), electric field strength and/or magnetic field strength in plasma ($\vec{E}$ and/or $\vec{B}$), plasma potential (V_p), intensity of current in the discharge (I_p), plasma particle collision frequency (ν_c), diffusion coefficient (D).

In general, the experimental diagnostic methods are classified into four main categories:

1. **Optical-spectral methods:** based on fundamental phenomena from spectroscopy or optics, such as: spontaneous emission of light, Thomson-Rayleigh scattering, the Doppler-Fizeau effect, the Stark effect, absorbtion of light, Bremsstrahlung radiation

   They are used routinely to determine the concentrations and temperatures of charge carriers and neutral particles in plasma.
2. **Electrical methods**: based on plasma response to low frequency signals or externally applied currents. Among the techniques belonging to this group of investigation methods we can enumerate the following: transducers, mass spectrometry, magnetic probes, electrical probes (Langmuir) or electron beam probing. The physical plasma parameters that can be determined with the help of the electrical methods are: concentration, temperature and energy distribution of charge carriers, electric field strength, magnetic field strength, intensity of current in the plasma column, plasma potential.
3. **High frequency diagnostic methods:** are diagnostic methods that are generally based on the use of electromagnetic signals from the microwave domain, and the response of the plasma to

these signals [3.8]. The main diagnostic techniques in this category are: microwave interferometry, Faraday rotation, cavity disruption method, resonant probe method.

4. **Non-thermal signal method**: is a method in which we analyze the electromagnetic signals emitted by the plasma. These signals are usually located in the radio or microwave domains.

3.1 The electrical characterization of the DBD type plasma generated with the "PLAS-01" generator

From the electrical point of view, the discharge chamber with the plasma column can be considered as an equivalent circuit consisting of two capacities (C_{d1} and C_{d2}) of the two layers of insulating material on the two electrodes, two capacities (C_{s1} and C_{s2}) of the plasma sheath layers (electron depleted layer in the immediate vicinity of the electrodes) and a resistance which is the resistance of the entire volume of plasma, R_{plasma}. The equivalent electrical circuit of the plasma + discharge chamber is shown in Figure 7. Using this electrical model and considering the phase shift angle between the current intensity and the applied voltage on the upper electrode of the discharge chamber, we can determine a series of parameters of the plasma.

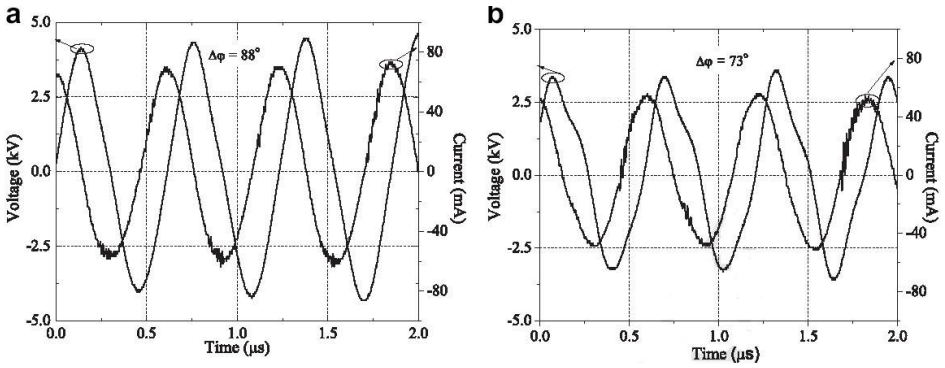

Figura 6. Waveforms for voltage and current on the active electrode of the chamber, **a**) – w/o ignited plasma, and **b**) – w/ the plasma ignited.

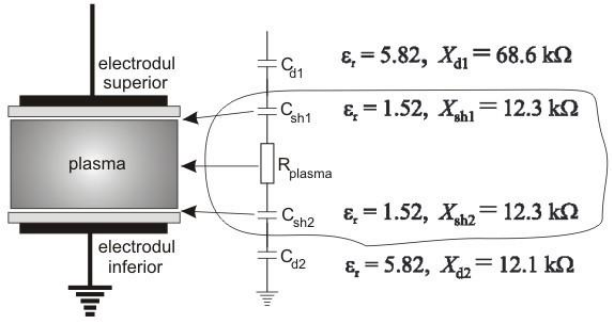

Figura 7. The model and the equivalent circuit of the DBD discharge chamber.

The calculated impedances are noted on the diagram in Figure 7. The thickness of the two plasma sheaths (electron depleted layers) was estimated to be d=0.08 mm. We also considered that the

thickness of these layers does not change during a period of the voltage waveform. The dielectric constant value of plasma sheaths was considered to be $\varepsilon_r = 1.52$ [3.8].

Considering the intensity of the current and the voltage as having an ideal sinusoidal shape, and knowing the amplitude of the applied voltage on the "active" electrode to be V_{p-p}=6.8 kV and considering a phase angle of 73 deg., the electrical resistance of the plasma column and the intensity of the current through the plasma will be given by equations (1) and (2):

$$R_{plasma} = \frac{X_{d1} + X_{d2} + X_{s1} + X_{s2}}{tg\varphi} = \frac{X_{total}}{tg\varphi} \tag{1}$$

$$I_{rms} = \frac{V_{rms\_electrod}}{\sqrt{R_{plasma}^2 + X_{total}^2}} \tag{2}$$

The current density in the plasma and the electron concentration is determined from equations (3) and (4):

$$j_e = \frac{I_{rms}}{A} \tag{3}$$

$$n_e = \frac{j_e}{e \cdot \mu_e \cdot E_{plasma}} \tag{4}$$

where: e is the electron charge

μ_e is the mobility of the electrons

E_{plasma} is the electric field strength inside the plasma volume.

The mobility of the electrons in Helium has the value of : 1128 $cm^2/(Vs)$, and:

$$E_{plasma} = \frac{I_{rms} \cdot R_{plasma}}{d_{plasma}} \tag{5}$$

where: $d_{plasma} = d_{gap} - 2 \cdot d_{patura\_plasma}$

The helium ion contributions to the total discharge current was ignored because they present a much lower mobility than the electrons.

The power density in the plasma column is given by equation (6):

$$p_{plasma} = \frac{I_{rms}^2 \cdot R_{plasma}}{A \cdot d_{plasma}} \tag{6}$$

The calculated values of these parameters are: $j_e = 45{,}5\,\mathrm{mA/cm^2}$, $n_e = 1{,}1 \cdot 10^{11}\,\mathrm{cm^{-3}}$, and $p_{plasma} = 101{,}8\,\mathrm{W/cm^3}$.

3.2 Diagnostics of the DBD type plasma generated with the „PLAS-02" generator

The studied high-frequency dielectric barrier discharge (DBD) (1.7 MHz) was generated using a discharge chamber containing two copper electrodes covered with dielectric material (Teflon), connected the the output of the "PLAS-02" power inverter circuit. The rectangular-shaped chamber has an internal volume of 160 cm^3 and it's made from heat resisting plexi-glass. The electrodes have a diameter of 24.5 mm and thickness of the teflon layers is 1.5 mm. The distance between them can be adjusted from 5 to 20 mm depending on requirements. The discharge chamber has a gas inlet port on one side and on the opposite side there are two 3 mm diameter holes for venting the chamber. The gas flow is perpendicular to the electric field generated between the two electrodes. The study was conducted at different power levels (1, 2, 5, 6, and 10 W) and at different gas flow rates (He), (0.15 to 3 l / minute). The schematic diagram of the experimental device is shown in Figure 8.

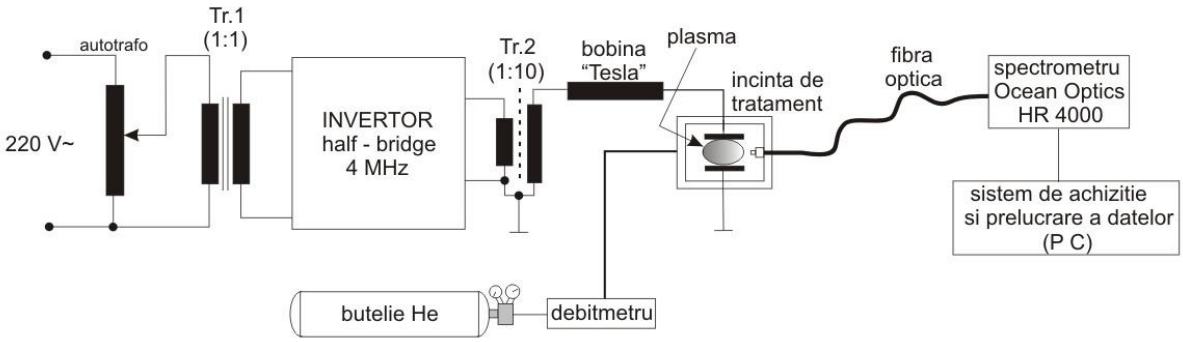

Figure 8. The schematics of the experimental system for the diagnostics work.

The absorbed power by the plasma was calculated with an accuracy of about 10%, using the method called "substraction". The electromagnetic radiation emitted by the plasma is focused on a sequencial monochromator slit which measures the intensity of emitted light at a given wave length domain. The entire measuring process and the data acquisition is controlled by a dedicated software called SpectraSuite [3.3]. The radiation emitted by the plasma was monitored using two Ocean Optics HR 4000 spectrometers (one for the spectral range of 290-430 nm with a resolution of 0.09 nm FWHM and one for the spectral range of 200-1100 nm with a resolution of 0, 5 nm FWHM). Our preliminary tests regarding the aspect of the plasma in the discharge chamber is shown on Figure 9. For a stable supply voltage ($U_{\pm} = \pm 86$ V) the plasma ignites at a helium flow of 0.4 l / min at which point we could observ its light emission (Figure 9 a).

At first we noticed that the discharge presents a thin column which covers only a small area of the electrodes, right in the middle. With the increasing of the He flow up to about 0.5 l / min, we

noticed an increase in the absorbed power and also an an increase in the electromagnetic radiation emitted by the plasma column (Figure 9 b).

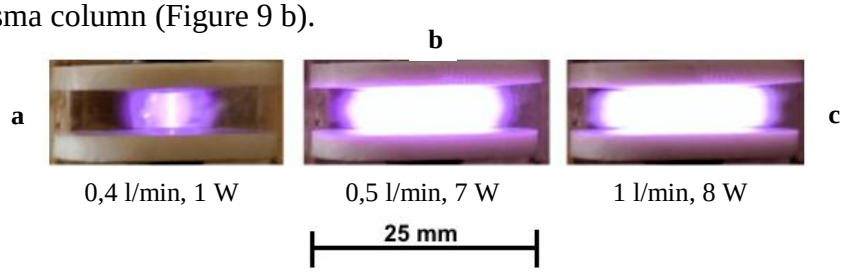

Figure 9. The generated DBD plasma in three different working modes.

At this point, the plasma column also increased in diameter and it almoust filled the entire space between the two electrodes. The shape of the discharge is cylindrical and it presents an intense purple-blue glow light. A further increase in helium flow up to 1.5 l / min results in an additional increase of the absorbed power and the intensity of light emitted by the plasma (Figure 9 c). For higher flow rates, we observed a slight decrease in the absorbed power, probably due to higher flow velocity of gas in the discharge area (Figure 10).

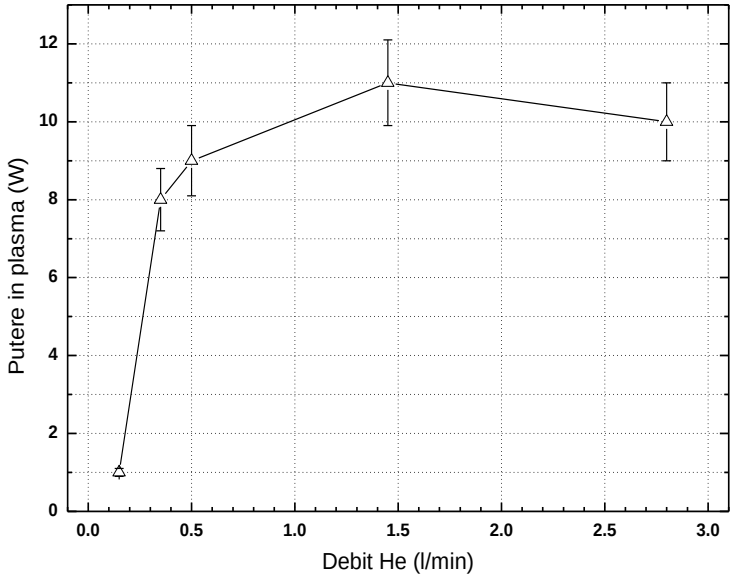

Figure 10. The power absorbed by the plasma as a function of the helim flow rate.

The graph which describes the appearance and the characteristics of the discharge based on voltage or power consumption and support gas flow, is called a ***stability diagram***. The diagram is very useful when we need to find the connection between the operating parameters of a plasma discharge and its different development stages. The first stability diagram was designed by Rezaaiyaan et al. [3.5] for an inductively coupled plasma. Their ideea and methodology was taken up by Forbes et al. [3.6] and Spencer et al. [3.7] who then both made diagrams of stability for all types of microwave plasmas (MIP and CMP). In case of the capacitive coupled RF plasmas, the first stability diagram was published in 2002 and 2005 respectively [3.7, 3.8]. So far, the literature does not provide information about the

stability diagram made for dielectric barrier discharges, thus the information below can be considered to be a first [3.9]. Such a stability diagram was made for the dielectric barrier discharge generated with the "PLAS-02" generator [3.2], in He at atmospheric pressure. For constant supply voltage values of the generator (between 0...120 V), the He flow was varied continuously from 0.1 l/min up to 6.0 l/min. The result of the visual observations has resulted in a chart which has four distinct regions, shown in Figure 11 along with some suggestive photographs of the various stages of development of the discharge. Thus, for He flow rates smaller than 0.3 l / min (regardless of the supply voltage) and supply voltages below 40 V (regardless of gas flow rates), the discharge cannot be ignited. This is marked on the stability diagram with the “white” area. The “○” simbols on the diagram represent the voltage and Helium flow pairs under which the breakdown occurs. After the breakdown, for a given supply voltage, any discrete increase in the gas flow will lead to the forming of a filamentary channel with purple-blue color. This is marked on the stability diagram with the gray area. The filament shaped discharge is formed on the central axis of the discharge chamber and has a diameter of approximately 1 mm.

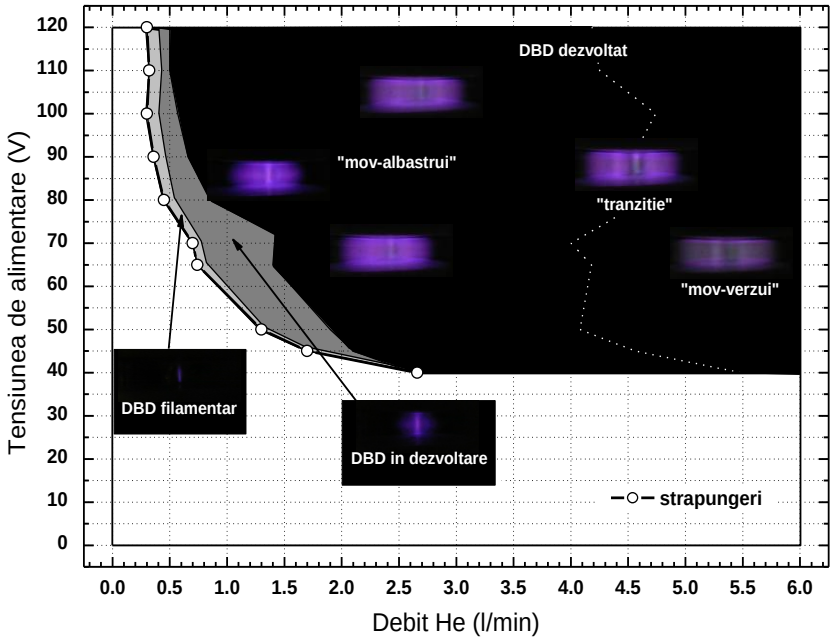

Figure 11. The “stability diagram” for the DBD plasma generated by the “PLAS-02” generator.

An aditional increase in the Helium flow will produce an expansion of the initial filament discharge. This deformation is more pronounced in the middle of the electrode area and less significant near the edges, making the discharge to resemble a ball shape. This is marked with the dark gray area on the chart. The plasma at this state has still a purple-blue colour and is in constant development, its size and appearance still depend on the gas flow.

The most important part of the diagram (colored in black) is the fully developed discharge state. Such a discharge can be obtained for small flow rates of He (around approx. 0.5 l / min) and supply voltages above 80 V or, lower supply voltages than 60 V and higher flow rates of He of 1.0 l / min. At this stage, the plasma tends to occupy the entire space between the electrodes: the central filament is surrounded by a dark space and a diffuse area (in cylindrical symmetry, their dimensions depend on both the voltage and the He flow). For flow rates of about 2.5…3.5 l/min, the discharge looks stable and has a purple-blue uniform colour, and it occupies almost the entire space between the electrodes, regardless of the supply voltage. For flow rates between 4.0 to 4.5 l/min, the plasma discharge is again discontinuous in its appearance (the central filament and a diffuse dark area) and tends to change its color: the filament begins to turn green, then, with an increased flow up to 6.0 l/min, the entire plasma column becomes purple-green.

The kinetic temperature of the homogenous discharge (75 V supply voltage and 1 l/min flow of helium) is approx. 513 K. This temperature was measured using a K-type thermocouple connected to a digital multimeter (Mastech M345). The thermocouple's measuring junction was previously covered with a layer of heat-resistant glass in order to avoid turning it into an auxiliary electrode when the thermocouple gets immersed in the plasma.

The evolution of the thermodynamic temperature of the gas and the vibrational temperature of N_2 molecule as a function of the supply voltage for a constant He flow of 1.5 l/min, is presented in Figure 12. As we expected, the gas temperature increases when the supply voltage increases because this leads to an increase in the plasma absorbed power. These values of the temperatures measured by thermocouple, are generally higher (up to 100 K higher) than the estimated rotational temperatures of the molecular emission spectrum given by the LIFBASE simulation software [3.4].

Thw vibrational temperature of the N_2 molecule decreases as the supply voltage increases. A plausible explanation for this evolution is the decrease of the total number of N_2 molecules in the excited state; this phenomenon is probably produced by the progressive dissociation of the N_2 molecules with the increasing of the absorbed power.

In order to find the optimal operating parameters (supply voltage and He flow) for various applications in the treatment of materials surfaces, we studied the composition of the plasma emission spectrum and its evolution as a function of the supply voltage of the generator and the flow of He.

The emission spectra of the various stages of development of the dielectric barrier discharge, obtained for a supply voltage of 110 V are shown in Figures 14 and 15. As we expected, the region in the spectrum corresponding to the wavelengths of UV is dominated by the species of nitrogen (□NO, N_2, N_2^+).

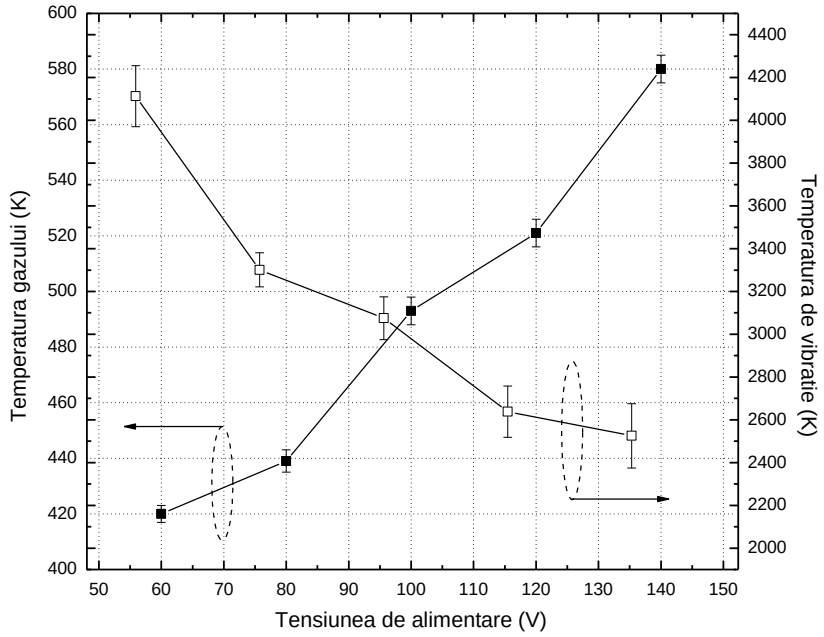

Figura 12. The kinetic gas temperature and the vibration temperature as a function of the supply voltage for a given He flow rate.

These molecular species come from the air that diffused in the plasma gas. In case of the wavelengths corresponding to the VIS spectrum, it can be seen that the lines are sparse, we only observed the helium line at 706 nm, and the lines of the hydrogen (at 656 nm) and oxygen (777 nm and 844 nm), the latter coming from the water vapor present in the air. The NO molecule present in the spectrum is the result of the chemical reaction between N and O, that occurs in the plasma, and the band corresponding to molecular nitrogen ion (N_2^+ at 391 nm) indicates the presence of the He metastable ions in the plasma discharge.

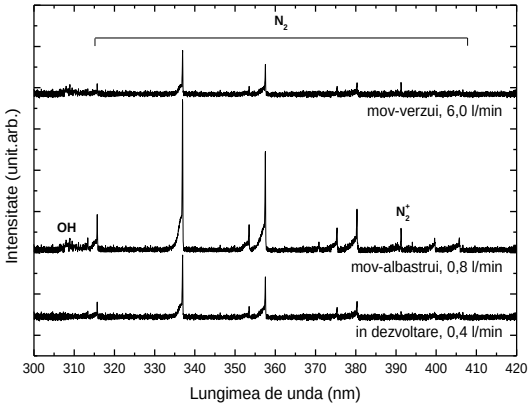

Figure 13. UV emission spectrum of the generated discharge.

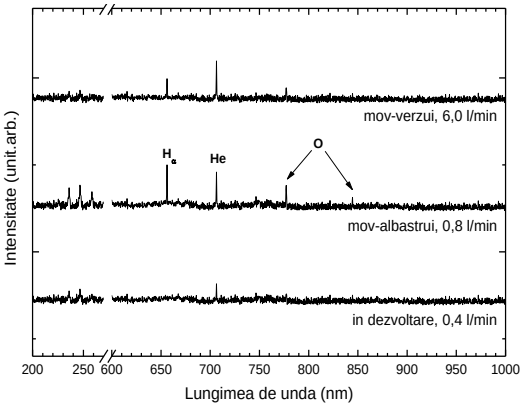

Figure 14. UV-VIS emission spectrum of the generated discharge.

Figure 15 presents the evolution of the emission of atomic and molecular species present in the plasma as a function of the supply voltage, at a constant flow of He of 1.6 l/min.

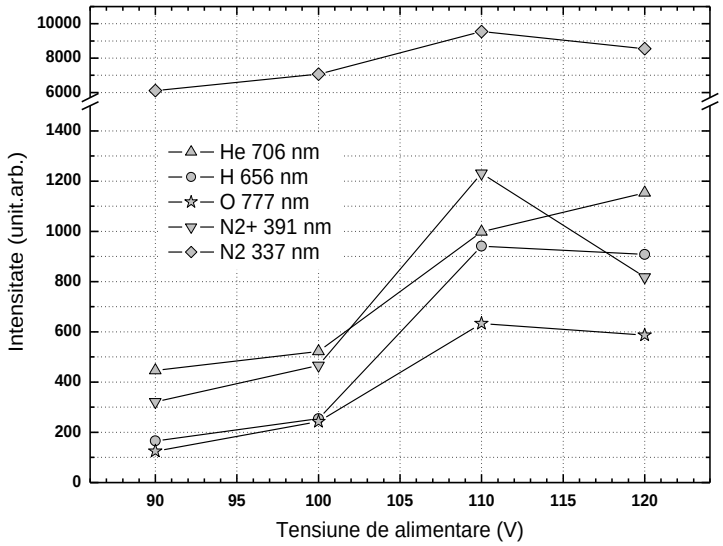

Figure 15. The evolution of the atomic and molecular species in the generated plasma as a function of the supply voltage, for a given flow rate of He of 1.6 l/min.

A careful analysis of this dependence leads to the conclusion that the value of the supply voltage of 110 V seems to be optimal for generating the active species with maximum efficiency for the surface treatment process. To be able to determine the optimal He flow rate He, we studied the evolution of the atomic and molecular emission of the species present in the discharge, as a function of the gas flow, maintaining a constant supply voltage of 110 V. The results are presented in Figure 16.

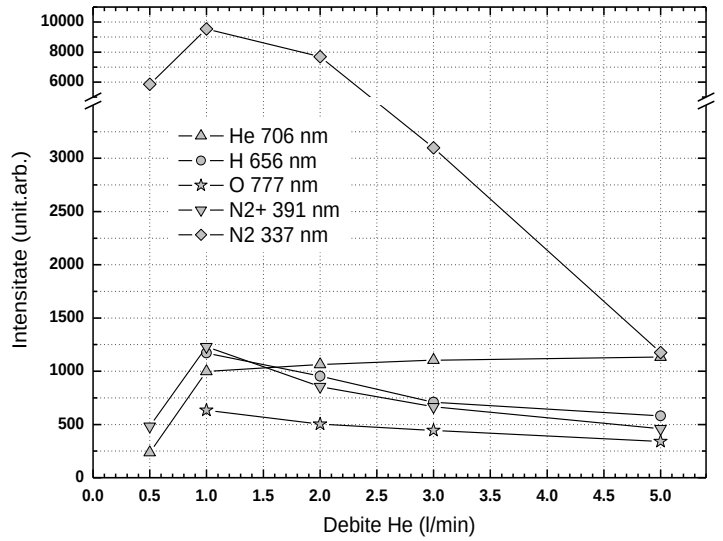

Figure 16. The evolution of the atomic and molecular species in the generated plasma as a function of the He flow rate, for a given supply voltage of 110 V.

Knowing that oxygen-containing species have key role in all processes in the plasma treatment of materials surfaces, we believe that the optimum He flow would be around l/min (maybe slightly

higher than this value) so that plasma discharge will function in a “fully developped” and homogenous state and also its emission lines from oxygen will be at a maximum.

References

[3.1] G. Popa, M. Gheorghiu, “Aplicaţii ale fizicii plasmei”, Ed. Univ. Al. I. Cuza, Iasi, 1998

[3.2] C.D. Tudoran, „Metode de generare ale plasmelor de înaltă frecvenţă”. Referatul nr.1 în cadrul programului de pregătire doctorală

[3.3] http://www.oceanoptics.com/products/spectrasuite.asp

[3.4] http://www.sri.com/psd/lifbase/

[3.5] Rezaaiyaan R, Hieftje G M, Anderson H, Kaiser H and Meddings B 1982 Appl. Spectrosc. 36 627

[3.6] Spencer B M, Smith B W and Winefordner J D 1994 Appl. Spectrosc. 48 289

[3.7] Simon A, Teză de doctorat, Universitatea Babeş-Bolyai, Fcaultatea de Fizică 2002

[3.8] Anghel S D, Simon A and Frentiu,” Characterization of a very low Ar CCP”, T 2005 J. Anal. At. Spectrom., 20, 966-973

[3.9] Simon A, Dinu O E, Papiu M A, Tudoran C, Papp J and Anghel S D 2011 Journal of Electrostatics – în curs de publicare

4. HIGH FREQUENCY PLASMA APPLICATIONS

Due to high portability and non-equilibrium nature of the discharge, non-thermal plasmas are increasingly studied in the recent years. The first experiments that used high-frequency cold plasmas were carried out during the '50s, but the development and study of plasmas at large-scale started after 1990 when the microelectronics and microtechnologies began their rapid development. Their general application domains include: bio-medical applications, plasma displays, sources of particles and/or ionizing radiation, chemical analysis systems, gas analyzers, photodetectors, lasers, microwave plasma dynamic processing equipment, chemical process reactors with cold plasma, propulsion systems, air flow control systems (with aerodynamic applications), materials processing and also environmental applications.

4.1 Modern applications of high-frequency plasmas

Besides the established applications of the low pressure plasmas, such as the fluorescent tubes, thin film deposition or plasma displays, in the last decade these types of discharges have found

theirselves several new applications in various scientific and technical domains, such as: treatment of textiles made from PET (**P**oly **E**thylene **T**erephthalate) in order to make them hidrophillic, titanisation of surgical implants, conservation of ancient artifacts made of iron, industrial manufacturing of multilayer printed circuit poard (PCB), DBD lasers with CO_2.

Applications of high frequency plasmas generated at atmospheric pressure in the biomedical field: polymeric biomaterials, polymer materials for vascular grafts, antimicrobial layers, plasma sterilization, inactivation of biofilms, inactivation of bacteria and proteins with plasma jets.

Technical applications of high frequency plasmas generated at atmospheric pressure: ozone generation, decontamination of gases, treatment of Diesel exhaust gases, treatment of volatile organic compound (VOC), catalytic oxidation of volatile organic compounds and methane in cold plasma reactors, industrial treatment of plastic foils

4.2 Contributions to sintering experiments of metalic powders in low pressure microwave plasma *)

The sintering process is a method for obtaining metal parts from metal powders or homogeneous mixtures of metal/ceramics by heating the material to a temperature lower than the melting point until the powder particles adhere to each other, forming a solid component (Figure 17).

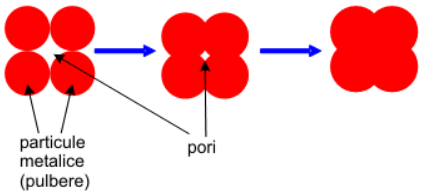

Figure 17. The principle of the sintering process.

The use of microwaves for processing metals is a relatively new technique. The most recent application relates to powder metal sintering by microwave plasma, a surprising application because the metals in solid form reflect the microwaves. In contrast, powdered metals absorb microwave energy and therefore they can be efficiently heated in the microwave field. Microwave plasma sintering is different from the conventional sintering method in terms of heat production in the sintered material. Conventional Sintering involves the heating of the workpiece by radiation or resistive effect, followed by transfer of heat within the component through heat conduction effect. In the case of plasma heating in microwave field, the heating effect is produced in volume. A comparative study between conventional sintering in gas oven and microwave plasma sintering was performed in order to highlight the superior mechanical properties of homogeneous mixtures of metal parts made from nickel -

*) This research was carried out at „University College Dublin" , School of Electric Electronic and Mechanical Engineering, Surface Engineering Group, Dublin.

diamond by microwave plasma sintering. In the test we prepared two equal groups of samples prepared from homogenous mixture of nickel and diamond powder; the samples were then subjected to the sintering process in microwave plasma generated in hydrogen at low pressure (20 mbar) and in a gas furnace. Nickel was chosen because it is a widely used metal in many domains and it has well known properties: high corrosion resistance, good resistance to mechanical wear, excellent electrical and thermal conductivity and has good magnetic properties. Nickel powders are commonly used as a binder component in applications where the use of refractory metals carbides and/or diamond is imposed, for example in the manufacturing of tungsten carbide cutter heads. The samples of nickel and diamond powder were obtained by uniaxial pressing in a cylindrical mold with a diameter of 20 mm under three compacting pressures: 100, 200 and 300 MPa. (Figure 18). The obtained bodie-densities in the three cases were: 52%, 58% and 62%. The density values were determined by two methods: direct measurement of the samples followed by weighing and by Archimedes' principle.

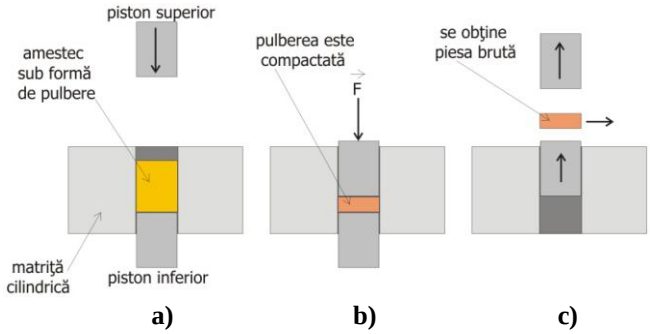

Figure 18. Manufacturing the powder metal samples: **a**) the powder is poured in the mold. **b**) the powder gets compacted under pressure, **c**) the crude sample is extracted from the mold.

After the sintering process, the samples were subjected to a series of mechanical tests: axial breaking effort, Rockwell hardness tests (Figure 19) and abrasion tests in order to prove the superior properties of the samples obtained by microwave plasma sintering.

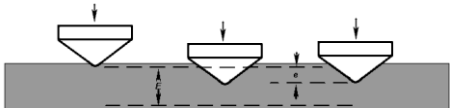

Figure 19. The principle of the Rockwell hardness test.

The abrasive wear tests were performed using the pin-on-disk method with a Teer POD-2 type machine, which has a tungsten carbide tip. The density measurement of the sintered samples showed an increase in the density by about 15% in both sets of samples, even though the sintering times were different: 10 minutes for plasma sintering and 8 hours in case of the furnace sintering. The axial breaking tests showed similar values in both sets of samples.

We noticed however that the samples pressed under high pressure (300 MPa) showed higher resistance when were sintered in plasma, and the samples which were obtained at low pressure (100 MPa) had higher strength properties when they were sintered in the gas furnace.

The hardness tests revealed that the samples sintered in plasma showed an increase in thesurface hardness on average by 34% compared to the samples sintered in the furnace for 8 hours. This difference in hardness is probably due to the much higher rate of temperature rise inthe microwave plasma, the samples reaching thermal equilibrium much faster, making the sintering process more efficient. The graph in figure 20 presents the results of the performed measurements (Rockwell harness and axial breaking strength).

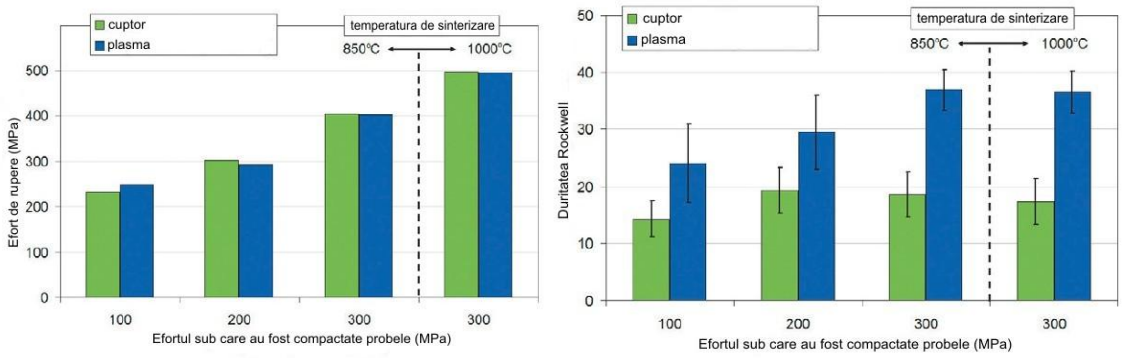

a **b**

Figura 20. The result of the breaking effort tests – **a)** and Rockwell harness tests – **b)**.

The metallographic microscopy images (Figure 21) showed that the plasma sintered samples have a finer and more homogeneous microstructure compared to samples sintered in the furnace. The samples sintered in the furnace have inhomogeneous areas where the nickel is present in excess, which confirms the lower hardness of this set of samples (greater porosity). The structural changes in the two cases can be explained if we consider the different rates of heating: 420 ° C/min. in plasma and 4^{o}C/min. in case of the furnace sintering. Also, the sudden cooling that occurs immediately after plasma extinction helps to obtain a finer grain microstructure.

In case of the pin-on-disk type wear tests (Figure 22 a) we compared the traces made by the tungsten carbide tip on each sample. After studying the obtained images (Figure 22 b) we noticed the presence of the tip material in the wear tracks, which indicated its erosion during the measurement. For this reason, a correct comparison between the two sets of samples was not possible.

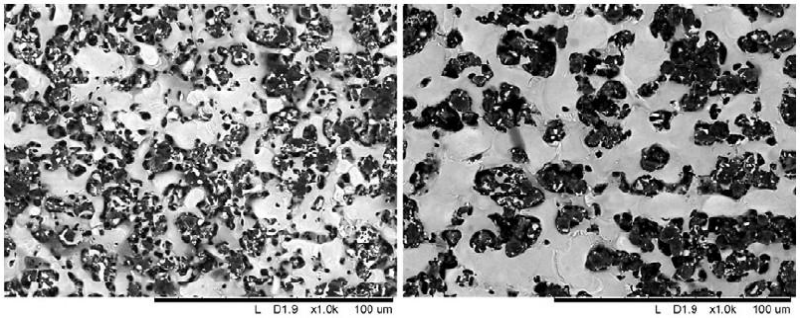

a **b**

Figura 21. Metalographic microscopy image of the sintered samples: a sample that was sintered in plasma – **a**), and a sample that was sintered in a gas furnace – **b)**.

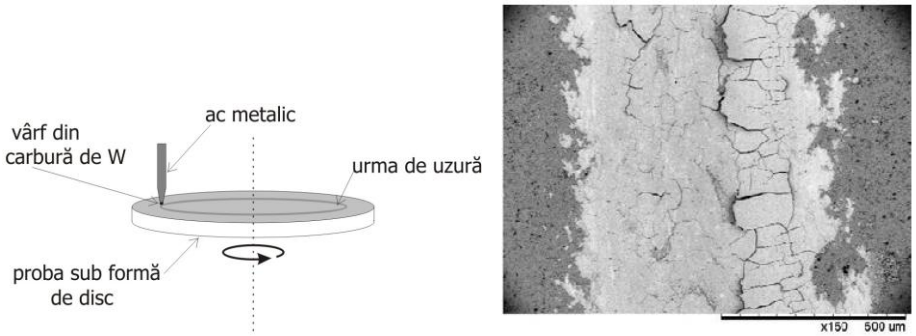

a **b**

Figure 22. The principle of the „pin-on-disc" abrasion test method – **a)** , the abrasion marks on the surface of one of the samples – **b)**.

Sintering of different metal powders in microwave plasmas generated in different gases

The purpose of this study was to find an optimal sintering algorithm (maximum temperature of the samples as a function of the plasma gas, input power and the type of material of the sample) for different samples of powdered metals. We chose to test four different metal powders with identical grain: cobalt, copper, stainless steel (type 316 alloy) and nickel. The set of samples was obtained using the same methodology as described in the preceding paragraph (uniaxial pressing in cylindrical mold under a pressure of 300 MPa) (Figure 22).

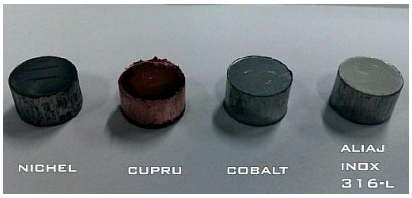

Figura 23. The metallic samples are ready to be sintered.

The sintering of the samples was performed in microwave plasma generated in four different gases: nitrogen, argon, oxygen and hydrogen. The conditions under which the plasmas were generated were kept constant in each of the four cases: pressure of 20 mbar, gas flow of 140 cm^3/min and the input power of 2.4 kW (2450 MHz). The tracked parameters in the test were the following: sample

temperatures – measured by two methods: optical pyrometer and S type thermocouple, plasma gas temperature – determined from atomic emission spectra (using Ocean Optics USB4000 spectrometers). The results of the temperature measurements recorded with a S type thermocouple are presented in Figure 24 a, b, c şi d.

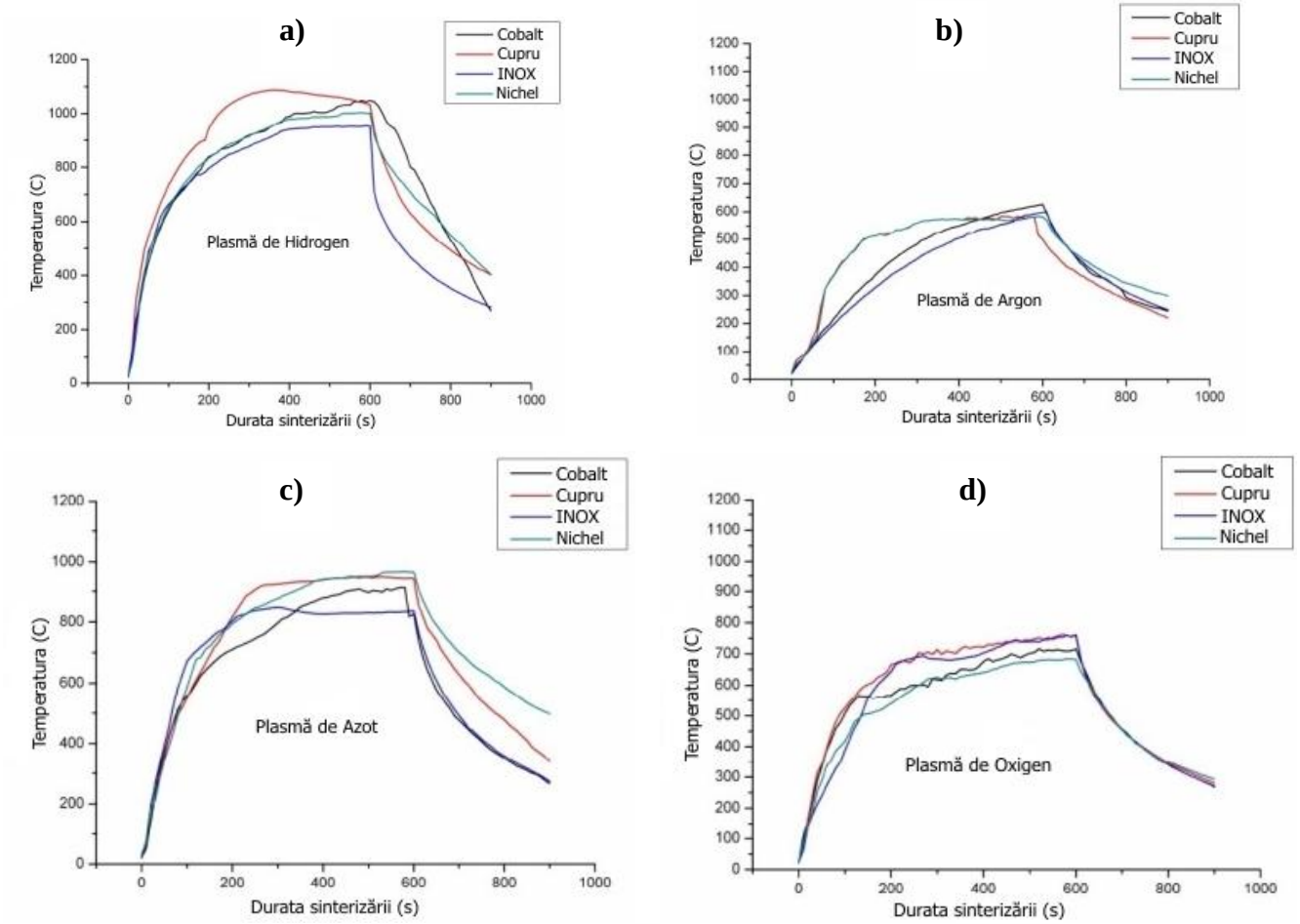

Figure 24. The results of the temperature measurements recorded with a S type thermocouple for the samples sintered in the following plasmas: **a)** – hydrogen plasma, **b)** – argon plasma, **c)** – nitrogen plasma, **d)** – oxygen plasma.

After this test, we determined the maximum temperature reached by each of the samples as a function of the plasma gas. After analyzing the data, we reached the conclusion that hydrogen plasma provides the highest sintering temperature and the highest rate of temperature rise. The study of the sintered metal microstructure for each sample was performed by metallographic microscopy.

The most homogeneous structure was observed for the cobalt, nickel and copper samples. Figure 25 presents the obtained metallographic microscopy images for the studied samples.

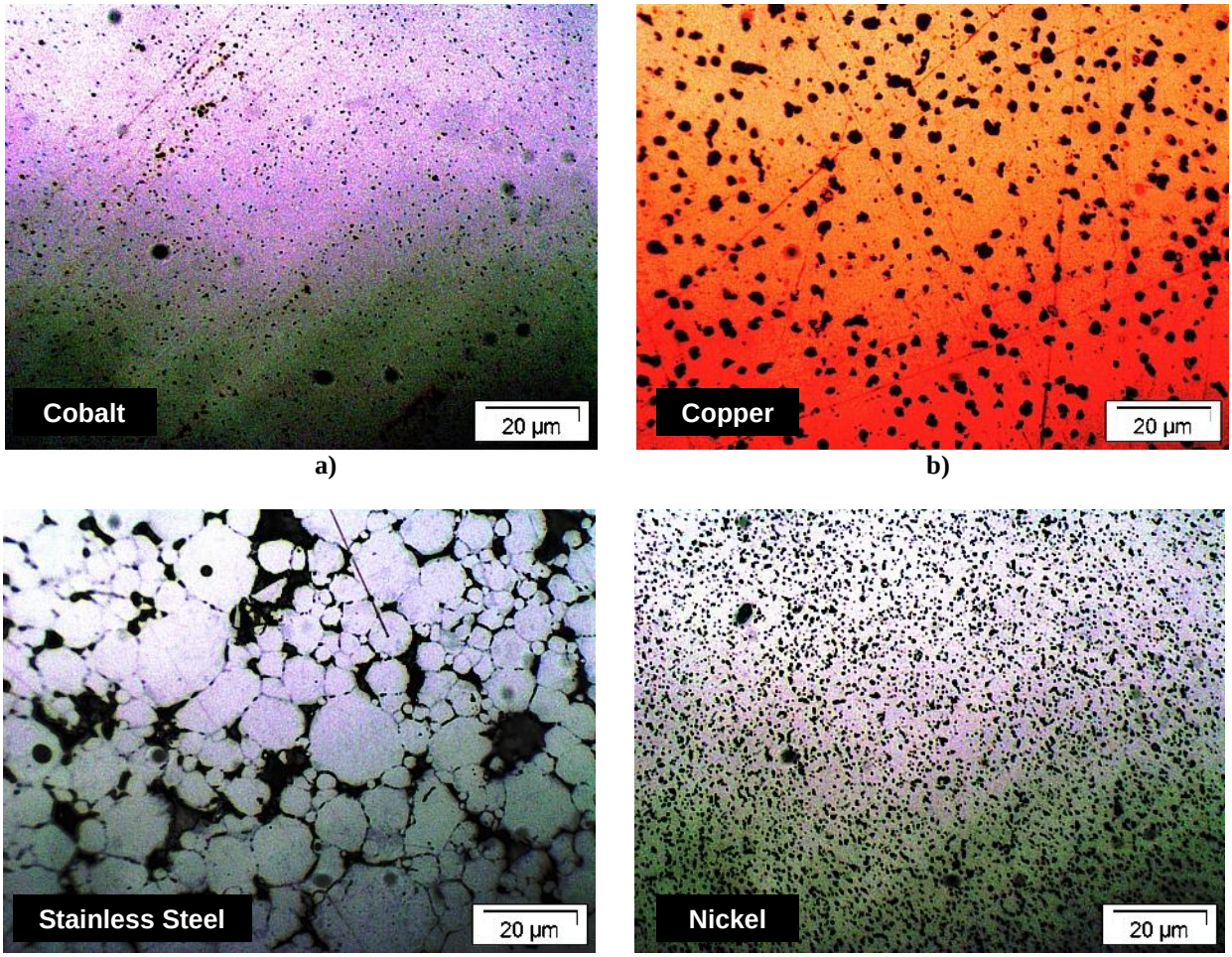

Figura 25. Metalographic microscopy of the studied samples: **a) –** cobalt, **b)** – copper, **c)** – stainless steel (alloy 316-L), **d)** – nickel.

4.3 Sterilization of *E.Coli* bacteria with the nonthermal high frequency plasma generated with the „PLAS-02" generator

The effect of the non-thermal plasma over the *Ecoli* bacterias is to significantly reduce plasma the viable populations present on glass surfaces (samples) for all combinations of power and He flow rates tested. Type *E.Coli* bacterias were initially developed on culture medias for 24 hours at a constant temperature of 37 °C. Then, the formed cultures were transferred under sterile conditions on a transfer medium with a neutral pH (7.0 pH). Next, a dilution of the sollution followed until the obtained sollution reached the desired concentration. On each glass slide a drop was deposited with a volume of 100 ml. After complete drying, the glass slides prepared in this manner, were subjected to non-thermal plasma treatment. After treatment, the suspension on the glass slides was washed with 5 ml of distilled water and 100 ml of the solution was transferred to a culture medium. Then followed another

incubation at 37 ° C for 24 hours and finally we counted the viable colonies. The number of colonies was compared with a reference set that was not exposed to the plasma treatment.

The effect of dielectric barrier discharge over the biofilm of *E.Coli* bacterias deposited on glass surfaces is shown in figure 26.

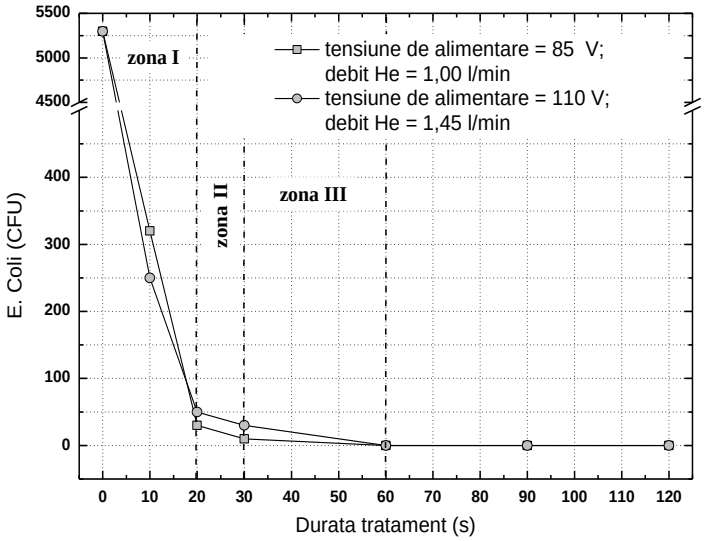

Figura 26. The inactivation effect of the nonthermal plasma on E. Coli bacterias.

We studied the number of formed colonies (CFU) depending on the duration of the treatment for two different operating conditions. The decimal reduction time and the time necessary to obtain a complete sterilization and destruction of microorganisms is presented in Table 1. It can be clearly seen that there are no significant differences between the two sets of experimental data on inactivation of E. coli bacterias. The inactivation process occurs with different speeds. For this reason the curves have three different slopes for the first 60 s of treatment. In the first 20 seconds the inactivation is a relatively fast process, with an average rate of destruction of about 500 CFU / s.

For the rest of the treatment, the sterilization process becomes even more slow: in the next 10 seconds the inactivation rate decreases by an order of magnitude (16 to 20 CFU / s), so that it becomes only 1 CFU/s in the interval of 30 - 60 s. Complete sterilization was obtained for a period of 60 s and the decimal time is 9-10 s.

Our results were comparable with the results obtained by: Sun et al. [4.5], Raymond et al. [4.6], Hippler et al. [4.7], Deng et al.[4.3], Stoffels et al. [4.2].

A possible future direction of research will be the study of the influence of inoculation methods on plasma performance to inactivate microorganisms: the use of more dilute cultures or mixed with other microorganisms, longer treatment times, etc.

Other interesting effects that can be studied are the interaction of two species of microoganisms which coexist with a layer of biofilm and the effect of cold plasma on these structures.

***Tabele 1**. The decimal reduction time and the time to complete sterilization as a function of the plasma parameters.*

Plasma operating conditions	**Initial concentration (CFU/ml)**	**Killing rate (CFU/s)**	**Decimal time (s)**	**Complete sterilization in (s)**
Supply voltage: 85 V He flow rate: 1,00 slpm	5300	zone I: 498 zone II: 16 zone III: 1	10	60
Supply voltage: 110 V He flow rate: 1,45 slpm		zone I: 505 zone II: 20 zone III: 1	9	60

The total surface of the discharge that covers the microbiological sample has a lower importance on the effect of inactivation than the plasma parameters and / or treatment times.

The differences in morphology observed in the discharge under different flow rates of Helium and absorbed power, such as: light emission, color, volume, dispersion, uniformity, appearance of filamentary discharges, shows that chemical composition (active species) and the physical properties of the discharge is determined by these parameters even if the chemical composition of plasma gas remained constant throughout the measurements. A higher flow rate of the plasma gas results in greater heat transfer to glass slides, high thermal conductivity due to Helium, but over a critical flow we observed the exact opposite effect, that the generated heat is dispersed in the volume of the discharge.

This effect is influenced by the geometry of the treatment chamber and the position of the gas inlet nozzle and also by the effect of turbulence that occurs at high gas flow speeds in the space between the two electrodes.

4.4 Rapid cleaning of glass surfaces with nonthermal high frequency plasma generated with the „PLAS-02" generator

Glass surfaces play an important role in modern technology such as automotive industry, semiconductor materials industry, manufacturing of hard drives or even in the field of microbiology. In the mentioned applications, obtaining clean glass surfaces is imperative.

There are several methods for the surface cleaning of glass, dust particles can be removed by compressed air, or they can be washed in an ultrasonic bath using organic solvents such as acetone, toluene, etc. [4.4].

Removal of the organic contaminant substances is carried out in general using chemical cleaning methods based on the use of acids or bases. All these methods have the disadvantage of using large quantities of toxic substances. Environmental protection and economic efficiency have imposed newer cleaning systems based on the effects of nonthermal plasmas.

The surface cleaning of glass surfaces using plasma, virtually eliminates the need to use organic solvents. Another advantage is the considerable reduction in the duration of the cleaning process. The effects of the nonthermal plasma cleaning process can also be used in the cleaning of silicon wafer surfaces, as the two materials have similar structure.

The glass surfaces treated in our experiments were characterized by contact angle measurements. The contact angle values were determined using a photographic method – the droplets deposited on glass surfaces were photographed before and after the plasma treatment, and then we used a dedicated software to determine the angles (ImageJ). As a test fluid we used double distilled water. As glass substrates we used microscope slides of 76 x 26 mm in size. The glass slides were cleaned with isopropyl alcohol before the plasma treatment. After the contact angle measurements, we obtained an angle 39.1^{o} before the treatment and an angle of 13^{o} after the plasma treatment (Figure 27 a and b).

a) **b)**

Figura 27. Water dropplets on the glass surface before plasma treatment - **a)** and after plasma treatment - **b)**.

For a He flow of 1 l/min and supply voltage of 40 V and 60 V respectively, the contact angle dependence of the duration of treatment is presented in Figure 28. There are no significant differences between the two sets of measurements, and the contact angle decreased from approx. 40° (control sample, untreated in the plasma) to 15° after a treatment time of only 2 seconds and then slowly to 13^{o} after another 3 seconds of exposure to plasma. This significant decrease in the contact angle was assumed to be the result of an effective cleansing of the glass surface. The results of the atomic force microscopy confirms indeed an effective cleaning and the lack of significant changes on the structure induced by the exposure to the non-thermal plasma (Figure 29 a, b and c). To highlight the durability of the effect of cleaning the glass surface in non-thermal plasma, we treated five sets of glass samples for 5 s in the plasma, then we recorded the evolution of the contact angles after 3, 24, 48, 72, 96, etc. hours after treatment. The graph in Figure 30 presents the test results. The error bars represent the standard deviation of five consecutive measurements. As it can be seen from the graph, the treated surface "ages" in time (it loses its properties), the contact angle begins to lose the initial value measured immediately after treatment (14^{o}) and begins to gradually return to pre-treatment value (39^{o}).

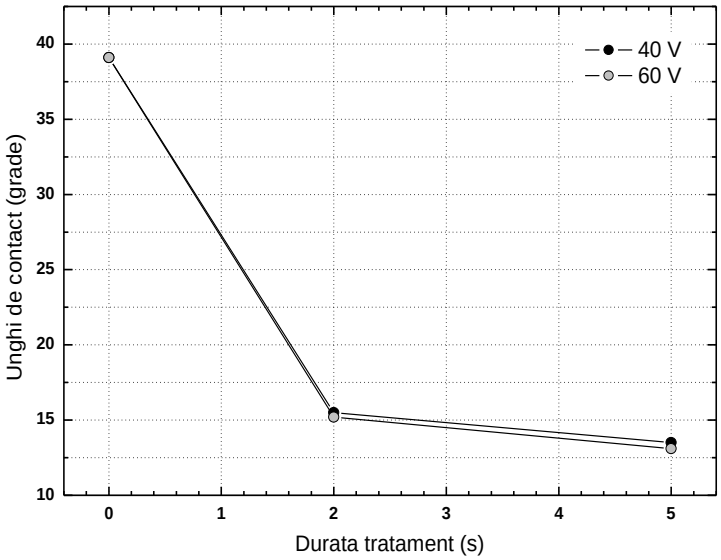

Figure 28. The values of the contact angles as a function of the plasma treatment time.

In conclusion, we can say that the first three hours after the surface treatment of the glass in the dielectric barrier discharge (DBD) are most favorable for their processing for later use (deposition of thin films, painting, plating, grafting, bonding, etc.).

To highlight the superior performance of the non-thermal plasma cleaning method for glass surfaces, we estimated the energy consumption of the system for treating a glass surface of 1 m^2, then we compared the result with the value obtained when using an ultrasonic cleaning bath, an Ultrawave type QS-12 [4.8], which has also an input power of 200 W. The ultrasonic cleaning bath has the option of heating the cleaning solution using an internal heating element of 250 W power.

The cleaning in the ultrasonic bath takes on average 5 minutes and when the heating of the solution is used, the cleaning time is reduced to only 1 minute. The results are presented in Table 2.

Tabelul 2 *Power consumption of the „PLAS-02" plasma generator compared to a Ultrawave QS-12 ultrasonic bath when cleaning 1 m^2 of glass surface.*

Technical parameters	**Nonthermal plasma cleaning**	**Ultrasonic cleaning (Ultrawave QS-12)**	**Ultrasonic cleaning + heating the cleaning solution (Ultrawave QS-12)**
Absorbed power, W	200 W	200 W	200 W + 250 W
Cleaning time of a single piece of glass, s	1 (36 mm x 28 mm)	300 (245 mm x 150 mm)	60 (245 mm x 150 mm)
Cleaning time for one m^2 of glass	1012 s / m^2	8086 s / m^2	1617 s / m^2
Total absorbed power, Ws/m^2	202 * 103 Ws / m^2	1617 * 103 Ws / m^2	728 * 103 Ws / m^2

As it can be seen from data presented in the table, using the high frequency non-thermal plasma cleaning method for glass surfaces, the treatment time is considerable reduced and the energy consumption is reduced by more than **3.6 times**.

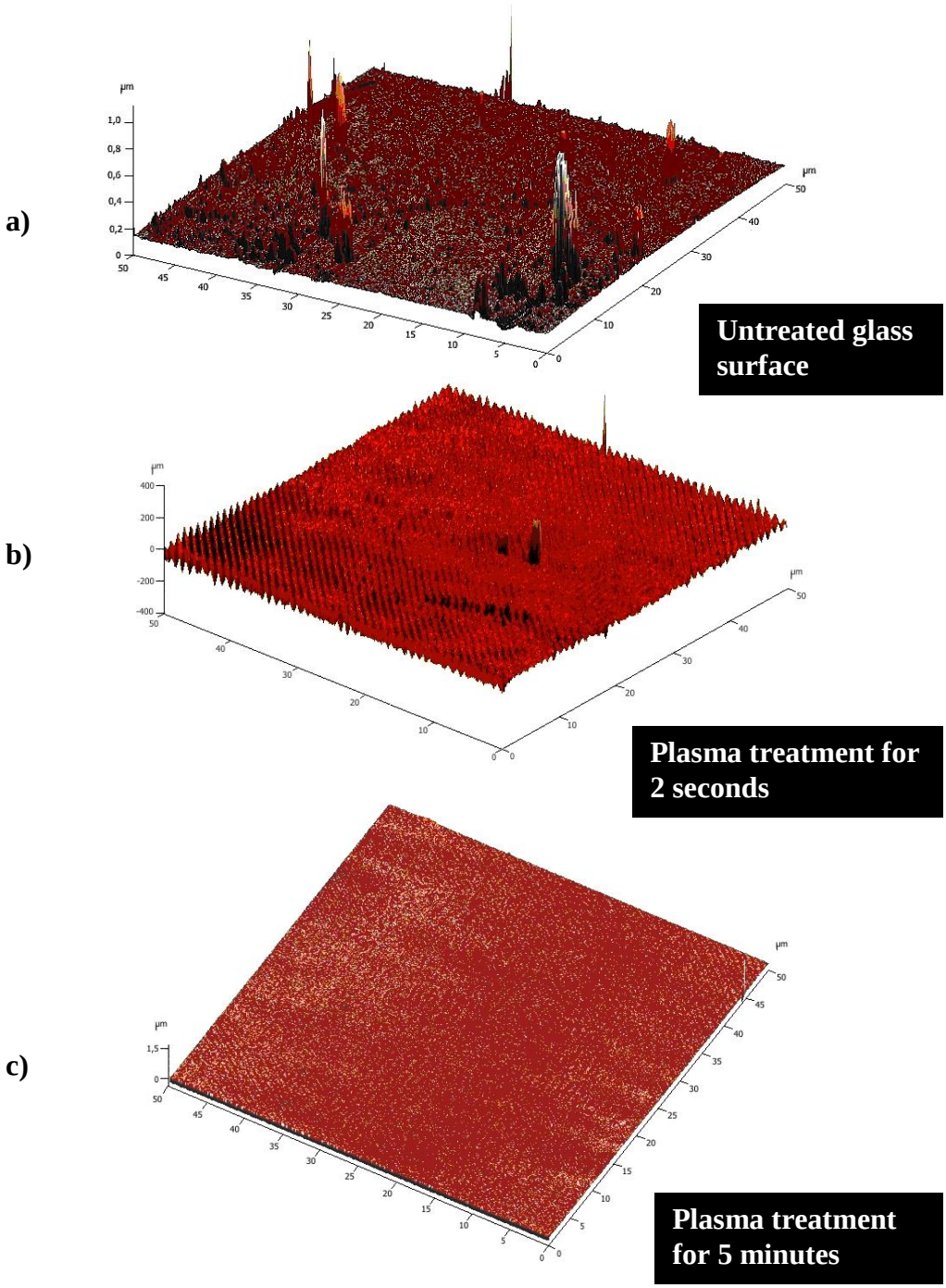

Figura 29. AFM pictures of the glass surfaces treated in nonthermal plasma. **a)** – untreated glass surface, **b)** – the glass surface after 2 seconds of plasma treatment, **c)** – the glass surface after 5 minutes of plasma treatment.

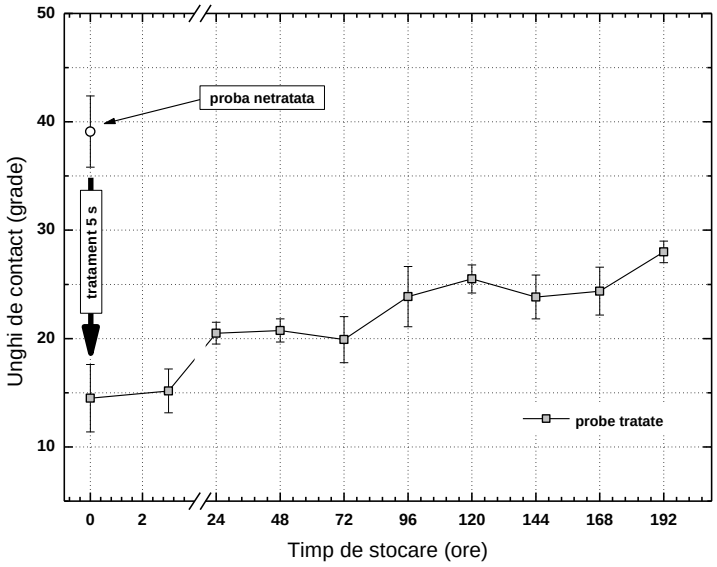

Figure 30. The variation in time of the contact angles.

References

[4.1] C.D. Tudoran, „Metode de generare ale plasmelor de înaltă frecvenţă”. Referatul nr.1 în cadrul programului de pregătire doctorală.

[4.2] S. Wieneke and W. Viöl, "Gas Lasers Excited by Silent discharge", Department PMF, University of Applied Sciences and Arts, von-Ossietzky-Str. 99, D-37085 Göttingen, Germany, 2000

[4.3] Shaobo Deng, Roger Ruan, Chul Kyoon Mok, Guangwei Huang, Xiangyang Lin, Paul Chen "Inactivation of Escherichia coli on Almonds Using Nonthermal Plasma", Journal of Food Science Volume 72, Issue 2, pages M62–M66, March 2007

[4.4] Andrej Bučeka, Tomáš Homola, Monika Aranyosiová, Dušan Veličb, Tomáš Plecenika, Josef Havelc, Pavel Sťahelc, and Anna Zahoranováa, "Atmospheric pressure nonequilibrium plasma treatment of glass surface", Chem. Listy 102, s1459−s1462 (2008)

[4.5] Sun Ja Kim, T. H. Chung, S. H. Bae, and S. H. Leem "Bacterial inactivation using atmospheric pressure single pin electrode microplasma jet with a ground ring", APPLIED PHYSICS LETTERS 94, 141502,2009

[4.6] Raymond E. J. Sladek, Eva Stoffels, Rick Walraven, Paul J. A. Tielbeek, and Ruben A. Koolhoven, "Plasma Treatment of Dental Cavities:A Feasibility Study", IEEE TRANSACTIONS ON PLASMA SCIENCE, VOL. 32, NO. 4, AUGUST 2004

[4.7] Abhijit Majumdar, Rajesh Kumar Singh, Gottfried J. Palm, and Rainer Hippler "Dielectric barrier discharge plasma treatment on E. coli: Influence of CH4/N2, O2, N2/O2, N2, and Ar gases", Journal of Applied Physics 106,084701,2009

[4.8] Fişa de prezentare a instalaţiei de curăţare ultrasonică „Ultrawave QS-12”
http://www.ultrawave.co.uk/products.php?id=15&cat=14&prod=73

5. CONCLUSIONS, ORIGINAL CONTRIBUTIONS, VALUEING THE RESULTS, PERSPECTIVES AND FUTURE WORK

5.1 General conclusions

After conducting the studies and analysis contained in this doctoral thesis, the following conclusions can be highlighted:

1. The RF plasma generators can be designed and built based on the effect of LC series resonant circuits using only general-purpose electronic components accessible to the public.
2. The radiofrequency plasma can be ignited and generated in the most easy way in Helium under atmospheric pressure conditions in a dielectric-barrier discharge chamber (DBD), which provides a laminar gas flow, which leads to a uniform and stable discharge.
3. The dielectric barrier discharge is stable in a wide range of supply voltages and Helium flow rates. Thus, with the discharge chamber we designed and built we managed to generate a discharge for any flow rate above 0.3 l/min. A stable functioning of the discharge was observed for flow rates between 0.5 and 6 l / min.
4. The stability diagram obtained for our high frequency dielectric barrier discharge (DBD) sustained at atmospheric pressure in Helium, has four distinct zones.
5. For higher flow rates than 1.5 l/min we noticed a slight decrease in the absorbed power by the plasma, due to the higher velocity of the gas flow in the discharge.
6. The kinetic temperature of the generated discharge increases linearly with the absorbed power reaching a value of about 300^{o}C for a power consumption of 10 W.
7. The vibration temperature of N_2 shows a decrease with the increasing of the plasma absorbed power at constant flow of He. This phenomenon occurs due to progressive dissociation of nitrogen molecules with the increased absorbed power.
8. In the characteristic emission spectrum of the generated dielectric barrier discharge we noticed the presence of emission lines of active molecular species (NO, OH, N_2^+, O), which is important in terms of the future applications for this type of plasma.
9. The entire volume of the dielectric barrier discharge has a resistive behavior.

10. From the electric point of view, the treatment chamber together with the plasma can be considered as a series RC circuit consisting of the capacities represented by the plasma sheats and the electrodes covered with dielectric material and connected in series with resistance R, represented by the volume of the discharge.
11. The microwave plasma sintering method for powdered metal materials provides a number of advantages over the traditional sintering process: reduced energy consumption and sintering time, high hardness surfaces, more homogenous structures.
12. After the performed sintering studies, we reached the conclusion that the hydrogen plasma provides the highest temperature for any given absorbed power level.
13. Among the studied metals, the most homogeneous structure was obtained for the cobalt, copper and nickel samples.
14. The dielectric barrier discharge generated at atmospheric in helium can be successfully used for disinfection and decontamination of surfaces containing biofilms of *E.Coli*.
15. The decimal time for an input power of 8W is approx. 9-10 s, and the complete destruction of biofilm was achieved after a plasma treatment duration of 60 s.
16. In terms of sterilization performance, the dielectric barrier discharge is comparable with the systems based on the effect of UV radiation.
17. The glass surfaces can be cleaned quickly and effectively in high-frequency non-thermal plasma. With the system we designed and constructed, we managed to obtain clean glass surfaces after only 2 s of exposure to the plasma.
18. The plasma cleaning method for glass surfaces provides a substantial reduction in energy consumption. Compared with the ultrasonic cleaning method, the plasma treatment provides an energy saving of about 3.6 times.
19. The plasma cleaning method also provides the advantage of eliminating the need to use volatile organic solvents in the cleaning process.
20. Our durability studies of the effect of the plasma in time revealed a progressive loss of the hydrophilic properties of glass surfaces after a period of approximately 192 hours from the treatment. For this reason, any further processing of the glass surfaces must take place within 3 hours after exposure to plasma.

5.2 Original contributions

The present thesis is structured in three main parts: *high frequency plasma generation*, *high frequency plasma characterization and diagnostics*, and *applications of high-frequency plasmas*. In each of these parts we highlighted the original contributions which resulted from the research we have conducted. These can be summarized as follows:

1. The CAD design, practical implementation (hardware) to the stage of prototype of the RF plasma generators "PLAS-01" and "PLAS-02".
2. Solving the problem of the control of the final power stage in the "PLAS-02" generator: given the typical operation conditions of the plasma generator (high voltages and currents at switching frequencies in the MHz domain) it was necessary to introduce a new separation technique between the drive modules and the power stages using fiber optic communications technology.
3. The use of resonance effects of the Tesla coils to generate high voltages required for igniting and maintaining the plasmas under atmospheric pressure conditions in different configurations (different geometries of the discharge chamber).
4. The design and implementation of the protection circuit for the "PLAS-02" generator, which has to follow in real-time the symmetric output voltage and output load current from the inverter in both half cycles of the signal. The protection circuit is based on ultra-fast comparators.
5. The posibility of the designed plasma generators to function at different frequencies, depending on the type of the load and discharge chamber geometry.
6. The use of the microwave plasma sintering technology for metal powders.
7. The stability diagram for the dielectric barrier discharge with generated with the „PLAS-02” generator. This diagram shows in a graphic manner the operating modes of the plasma depending on a series of physical parameter: supply voltage, input power, plasma gas flow rate. The igniting conditions of the plasma are presented and the development of the discharge in time as a function of the physical working parameters.
8. The diagnostics of plasmas generated using the „PLAS-01” and „PLAS-02” generators.
9. The testing of the dielectric barrier discharges generated with the „PLAS-01” and „PLAS-02” generators in the inactivation of *E.Coli* type bacterias and in the cleaning of the glass surfaces.

5.3 Published or waiting to be published papers

1. **C.D. Tudoran**, Simplified portable 4 MHz RF plasma demonstration unit., IOP Publishing, Journal of Physics, Conference series nr. 182/2009, doi:10.1088/1742-6596/182/1/012034
2. **C.D. Tudoran**, High frequency portable plasma generator unit for surface treatment experiments, Romanian Journal of Physics, volum. 56/2011, pag. 103
3. **C.D. Tudoran**, V. Surducan, A. Simon, M.A. Papiu, O.E. Dinu, S.D. Anghel, High freruency inverter based atmospheric pressure plasma treatment system, Romanian Journal of Physics – în curs de publicare.
4. A. Simon, O.E. Dinu, M.A. Papiu, **C.D. Tudoran**, J.Papp, S.D. Anghel, Atmospheric pressure dielectric barrier discharge plasma obtained in flowing Helium at 1.74 MHz frequency, Journal of Electrostatics – în curs de publicare.
5. **C.D. Tudoran**, V. Surducan, S.D. Anghel, High frequency atmospheric cold plasma treatment system for materials surface processing, American Institute of Physics – în curs de publicare.
6. A. Simon, O.E. Dinu, M.A. Papiu, **C.D. Tudoran**, S.D. Anghel, Ageing behaviour of DBD treated glass surface, Romanian Journal of Physics – în curs de publicare.

5.4 International conferences

1. Processes in Isotopes and Molecules, 29 Sept – 01 Oct 2009, Cluj-Napoca, România – poster, **C.D. Tudoran**, „Simplified portable 4 MHz RF plasma demonstration unit".
2. International Conference on Plasma Physics and Applications, 1 – 4 Iulie 2010, Iaşi, România – poster, **C.D. Tudoran,** „High frequency portable plasma generator unit for surface treatment experiments".
3. International Balkan Workshop on Applied Physics, 6 – 8 Iulie 2011, Constanţa, Romania, - poster, **C.D. Tudoran**, V. Surducan, A. Simon, M.A. Papiu, O.E. Dinu, S.D. Anghel „High freruency inverter based atmospheric pressure plasma treatment system".
4. Processes in Isotopes and Molecules, 29 Sept – 01 Oct 2011, Cluj-Napoca, România – poster. – **C.D. Tudoran**, V. Surducan, S.D. Anghel, „High frequency atmospheric cold plasma treatment system for materials surface processing".

5.5 Perspectives and future work

The targets in the future are the solving of the practical problems associated with the high frequency energy transfer to the plasma, the development of optimal geometry discharge chambers and the study of the effects of a series of physical factors (external static or variable magnetic field, special mixtures of gases, the presence of neutral particles in the plasma, etc.) on the behavior of non-thermal plasmas and their effects on various materials. A novelty in terms of the scientific laboratory equipment with applications in surface engineering is the facility of the plasma generators to allow the treatment of samples without the use of special treatment chambers, through the use of a fine control for the power output and the gas flow.

Acknowledgement

In the first place I would like to record my gratitude to Prof. Dr. Sorin Dan ANGHEL for his supervision, advice, and guidance from the very early stage of this research as well as giving me extraordinary experiences through out the work. Above all and the most needed, he provided me unflinching encouragement and support in various ways.

I gratefully acknowledge Conf. Dr. Simon Alpár for his advice, supervision, and crucial contribution, which made him a backbone of this research and so to this thesis.

Many thanks go in particular to Dr. Eng. Vasile Surducan and Dr. Eng. Emanoil Surducan from the National Institute for Research and Development of Isotopic and Molecular Technologies, Cluj (*I.N.C.D.T.I.M* Cluj – Napoca) for their valuable advices in the design of the radiofrequency plasma generators.

I also whish to say thanks to Dr. Judit Papp from Faculty of Biology and Geology from Cluj and to my colleagues Mihaela Papiu and Otilia Dinu for her help in the plasma sterilization experiments.

Many thanks go to Dr. Dennis P. Dowling and to my coleague Aidan Breen from University College Dublin, Surface Engineering Group for their help with the sintering experiments.

An finally I would like to say thank my colleagues Dr. Diana Bogdan and Drd. Cozar Bogdan from the National Institute for Research and Development of Isotopic and Molecular Technologies, Cluj (*I.N.C.D.T.I.M* Cluj – Napoca) for their help with the AFM study of the plasma treated glass surfaces.